Slow migration of mobilised fines during flow in reservoir rocks: Laboratory study

Maira A. Oliveira [a], Alexandre S.L. Vaz [a], Fernando D. Siqueira [a], Yulong Yang [b], Zhenjiang You [b], Pavel Bedrikovetsky [b,*]

[a] Laboratory of Exploration and Production Engineering LENEP, North Fluminense State University UENF, Macaé, RJ, Brazil
[b] Australian School of Petroleum, The University of Adelaide, 5000 SA, Australia

A B S T R A C T

Permeability decline during high rate flows has been widely reported for corefloods and for production wells. The phenomenon is attributed to mobilisation of fine particles at elevated velocities, their migration in porous space with the following straining in thin pores and attachment to pore walls. Sixteen sets of corefloods with piecewise constant rate have been performed under increasing flow rate. The particularities of this study are long injection periods, allowing estimating permeability stabilisation times, and pressure measurements in intermediate core points, permitting for evaluation of the permeability profile variation along the core. It was found out that the mobilised particles drift with speeds significantly lower than the carrier fluid velocity, resulting in long permeability stabilisation periods.

© 2014 Elsevier B.V. All rights reserved.

1. Introduction

Detachment of the reservoir fines, their migration as colloids or suspensions in the carrier fluid with further straining in thin pore throats and attachment to pore walls occur in numerous petroleum production processes. The main features of the processes are the variation of colloidal suspension concentration in carrier fluid, which is important for produced water disposal in aquifers, and the permeability decline affecting well productivity and injectivity (Civan, 2007; Rousseau et al., 2008; Byrne and Waggoner, 2009). The above occurs during filtrate invasion into reservoirs during well drilling (Schechter, 1992; Watson et al., 2008), fines migration in oil and gas reservoirs (Schembre and Kovscek, 2005; Civan, 2007) and low quality water injection into oilfields (Nabzar et al., 1996; Pang and Sharma, 1997; Chauveteau et al., 1998). The role of fines migration during low-salinity waterflooding of oil reservoirs is a subject of the current intensive research (Tang and Morrow, 1999; Morrow and Buckley, 2011; Zeinijahromi et al., 2011; Yuan and Shapiro, 2011; Hussein et al., 2013). The permeability reduction due to fines migration can be used for water production control (Zeinijahromi et al., 2012). The list of fines migration applications can be significantly expanded.

The common view on the flow of mobilised fines in porous reservoirs is that the fine colloidal or suspension particles are transported in the carrier fluid. It means that the advective velocity of particles is equal to the carrier fluid velocity; the permeability stabilisation occurs after arrival of the "last" mobilised fine at the core outlet, i.e. after the injection of one pore volume. Several authors have mentioned the two-speed structure of the colloidal suspension flux, where the particles may undergo the near-surface motion with significantly reduced speed if compared to the carrier water velocity (Yuan and Shapiro, 2010). The particle drift near the rough pore walls as modelled by Navier–Stokes equations has the speed significantly lower than the injected water velocity (Sefriouri et al., 2013). However, the vast majority of mathematical models assume equality of particle and water velocities (Bradford et al., 2008, 2009). Besides, laboratory studies of slow fine particle migration in porous media are not available in the literature.

Several laboratory corefloods with increasing velocity in order to lift fines have been performed, yielding the clear understanding of mobilisation and straining phenomena (Priisholm et al., 1987; Ochi and Vernoux, 1998; Kuhn et al., 1998, etc.). The detailed overviews of those works are presented by Tiab et al. (2004) and Civan (2007). Yet, the permeability stabilisation periods cannot be evaluated from the results of these tests due to short injection times. Also, the permeability profile cannot be evaluated since only the pressure drop across the overall core has been measured.

In the current work, the corefloods with piecewise constant velocity in the mode of velocity increase in order to lift the natural

reservoir fines are performed until the permeability stabilisation. It is found out that the permeability stabilisation periods significantly exceed one pore volume injected in all the tests, while the assumption of equality of particle and water velocities yields the stabilisation after injection of one pore volume. The delayed stabilisation is attributed to slow fines transport near pore walls. The stabilisation time decreases with the flow rate increase, which is explained by simultaneous increase of drag force driving the particles along the rock surface.

The structure of the paper is as follows. Brief physical description of colloidal suspension transport in porous media is given in Section 2. Section 3 presents the details of the laboratory set-up, rocks and fluids used and the methodology of laboratory tests. The test results are presented in Section 4. The paper is concluded by the discussions of results (Section 5), where the observed phenomena of delayed permeability stabilisation are attributed to the slow particle drift along the rock surface.

2. Physics of fines mobilisation, migration and straining

Following Muecke (1979), Sharma and Yortsos (1987), Chauveteau et al. (1998), Bergendahl and Grasso (2000), Freitas and Sharma (2001), Byrne et al. (2010), Bradford et al. (2011) and Bedrikovetsky et al. (2011, 2012), let us describe the main physical factors determining fines migration with consequent permeability decline in porous media. Detachment of fine particles, their migration with followed straining or attachment is shown in Fig. 1. The mobilised fine particle is retained by size exclusion if its size exceeds the pore size (Yuan et al., 2012; You et al., 2013). The fine particle intercepting a grain can also be attached, if there are available attachment sites on the grain surface. The forces exerting upon a single particle attached to the grain are shown in Fig. 1. The particle on the grain surface or on top of the internal cake formed by other attached particles is subject to electrostatic, drag, lifting and gravitational forces. The particle is attached if the attaching torque of electrostatic force and gravity exceeds the detaching torque of drag and lifting forces; otherwise the particle leaves the grain surface. The torque equilibrium is the condition of the particle mechanical equilibrium. The electrostatic force depends on the grain–particle disjoining distance that reaches the maximum at certain disjoining distance value. For the given values of drag, lifting and electrostatic forces, particle mobilisation is controlled by the maximum value of the attractive electrostatic force. If the attaching torque exceeds the detaching torque, the disjoining distance is determined by the torque balance under given values of drag, lifting and electrostatic torques. From the torque balance criterion follows that under the mechanical equilibrium, there does exist the maximum concentration of retained particles that is a function of carrier fluid velocity, salinity, pH, temperature, etc. Particle detachment due to velocity, pH or temperature increase or salinity decrease is described by the maximum retention function decrease. Velocity increase yields an increase of drag and lifting forces; it may raise the detaching torque resulting in the particle mobilisation. The water salinity decrease causes a decrease of the electrostatic force with consequent decrease of the attaching torque and fines mobilisation. Increase of temperature and pH also causes weakening of electrostatic force with consequent fines mobilisation. The above phenomena of fines mobilisation by increasing velocity have been observed and discussed in laboratory studies by Miranda and Underdown (1993), Ochi and Vernoux (1998), Bradford et al. (2011), while the fines lifting due to salinity decrease or temperature and pH increase is presented by Lever and Dawe (1984), Sarkar and Sharma (1990), Valdya and Fogler (1992), Khilar and Fogler (1998) and Civan (2010).

The classical filtration theory introduces critical velocity as the minimum velocity, where fines mobilisation occurs (Miranda and Underdown, 1993). Critical salinity is the salinity threshold below which the fines are lifted (Khilar and Fogler, 1998). The particle detachment rate is proportional to the difference between the current and critical values of velocity, salinity, pH, etc. The proportionality coefficients correspond to relaxation times, which are empirical coefficients and are obtained from the fitting. The model exhibits the delay in permeability response to an abrupt change of the parameters, while several laboratory studies reveal an instant permeability response (Lever and Dawe, 1984; Ochi and Vernoux, 1998; Bedrikovetsky et al., 2012). The above mentioned model of maximum retention function is free of this shortcoming.

If the migrating particle intercepts the grain and the attaching torque exceeds the detaching torque, the particle becomes attached to the grain. The size exclusion mechanism of the particle has been mentioned before. Another mechanism of particle retention is diffusion into the dead-end pores, where the particles may remain not being accessible to the flow in skeleton pores. In the next section we present the methodology and set-up of the laboratory study of fines mobilisation under increasing flow velocity followed by migration and capture.

3. Laboratory study

In this section we describe laboratory set-up (Section 3.1), characteristics of rock and fluids (Section 3.2) and methodology of flow testing under alternate velocities (Section 3.3).

3.1. Set-up

The schematic of laboratory set-up with specification of all key elements is shown in Fig. 2. Fig. 3 is the photo of set-up. The injected fluid is placed in Beaker 1 and is injected by PU-2087 pump Jasco under constant rate. The core-holder Mantec (Labconte) with two intermediate ports for pressure measurements is controlled by valves 14 and 15. The overburden pressure in coreholder is provided by manual pump Fluke 10 and is monitored by manometer 11. Pressure transducers 5, 6 and 7 measure pressure drops across the overall core, between the entrance and second ports and across the first core section, respectively. The Yokogawa transducers are calibrated to measure the pore pressure from zero to 500 psi. The data acquisition system 8 delivers a digital form for
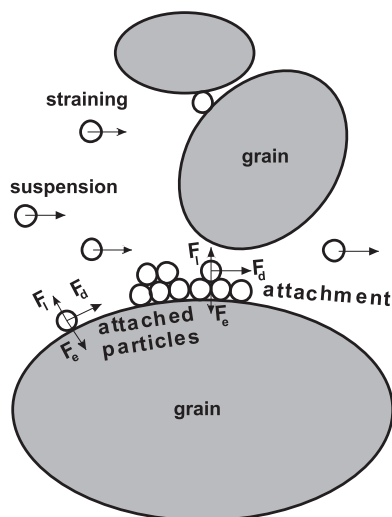

Fig. 1. Fine particles detachment from grains, migration in carrier water, attachment to grains and straining in thin pores.
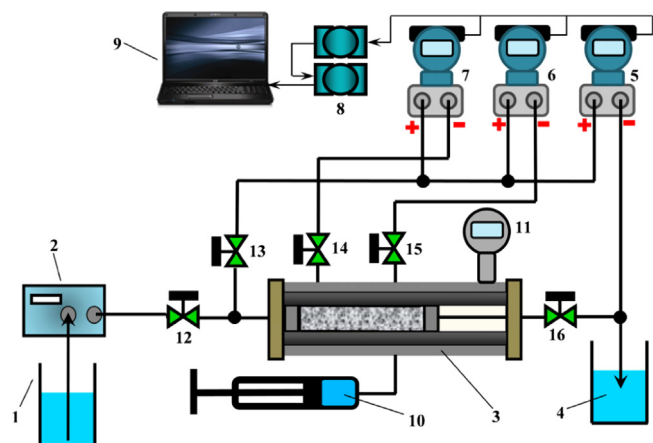
Fig. 2. Schematic of laboratory set-up for fines migration in porous media: 1 – injected fluid, 2 – pump, 3 – core-holder with core, 4 – produced fluid, 5,6, 7 – pressure transducers, 8 – data acquisition system, 9 – PC with LabView, 10 – manual pump to maintain overburden pressure, 11 – manometer, 12–16 – control valves.
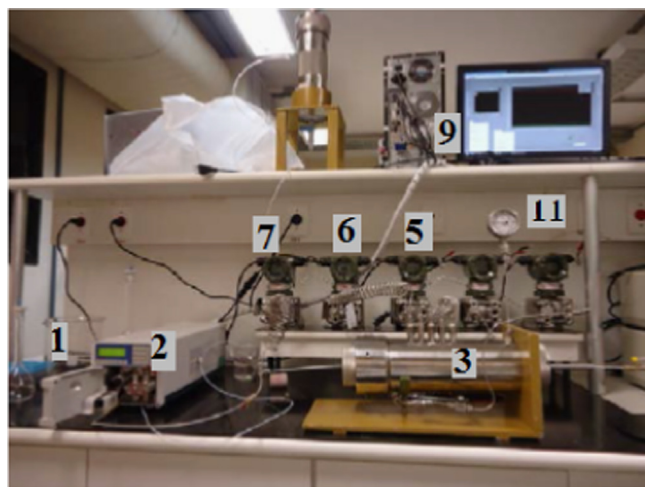

Fig. 3. Set-up for investigation of fines migration in porous media.

the measurements of three pressure transducers and transfers it to PC 9. The data are treated by the software LabView installed in PC. The effluent fluid is collected in Beaker 4 for further electrical resistance, pH, breakthrough concentration and fine particle size distribution measurements.

3.2. Core and fluid

Corefloods in 16 Berea cores with alternate velocities have been performed. Some core and brine properties for Core 12 are presented in Table 1. Table 2 shows initial core permeability and brine salinities for 16 tests. The cores 8–20 and 21–24 have been cut from two different blocks. The permeability values in the first block are lower than those in the second block. Cores have diameters determined from the core-holder size – 0.038 m. Core length varies from 0.044 to 0.072 m. Fresh Milli-Q type ultrapure water has been used for preparing the solution of sodium chloride. The brine has been filtered using 0.22 µm filter.

3.3. Methodology of laboratory study

In order to determine porosity, dry cores are weighted, saturated by brine with a determined salinity under vacuum and

weighted again. Dry Berea core has been saturated by brine at low velocity (at the injection rate 0.5 mL/m). The salinity varies from test to test from 6 to 30 g/L. The brine pH is below 7 (Table 1). The

Table 1
General water and core data for Test 12.

Parameter	Test 12
Salinity	10.0 g/L NaCl
pH	6.4
Total core length	7.2 cm
Intermediate point core length	0.7 cm and 2.9 cm
Porosity	19%
Cross-sectional area	11.53 cm^2
Solution viscosity	1.0 cP
Initial permeability	58 mD

Table 2
Stabilised times in different tests.

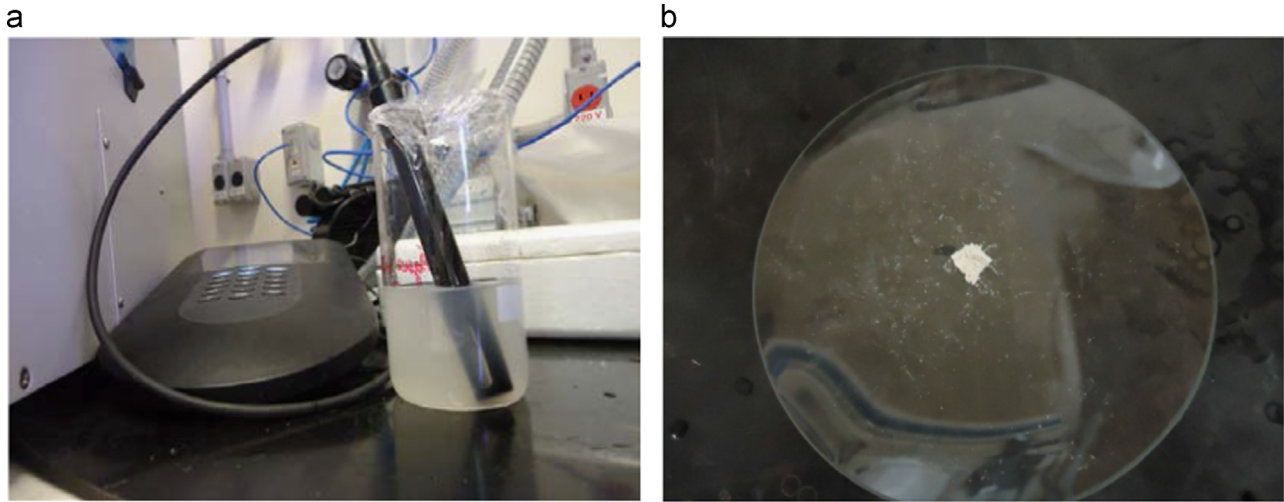| Test no.	K_0 (mD)	Q (ml/min)	Duration of tests (pvi)	Stabilisation time (pvi)	Brian salinity (g/L)	K_{st} (mD)
8	57	10	303	20	10	40
		20	595	16	10	36
		30	585	20	10	32
9	70	10	281	16	10	61
		20	623	14	10	55
		30	706	18	10	50
10	44	10	200	16	6	38
		20	505	15	6	33
		30	778	20	6	31
11	30	10	18	16	10	30
		20	469	20	10	27
		30	710	14	10	26
12	58	10	91	25	10	31
		20	361	17	10	26
		30	455	30	10	24
13	61	10	127	11	30	42
		20	752	19	30	35
		30	563	22	30	32
14	44,9	10	146	14	30	40
		20	628	17	30	34
15	56	10	123	14	10	46
		20	451	23	10	38
		30	485	15	10	34
16	50	10	129	14	6	39
		20	420	20	6	33
		30	527	20	6	30
18	60	10	133	27	6	43
		20	599	23	6	35
		30	803	18	6	34
19	71	10	146	23	6	45
		20	595	25	6	36
		30	627	19	6	31
20	75	10	120	12	10	32
21	270	10	72	19	10	173
		20	306	18	10	155
		40	421	21	10	122
		48	450	23	10	118
22	109	5	44	13	10	106
		10	97	18	10	84
		15	213	12	10	71
		20	198	10	10	67
		25	367	11	10	59
		30	1278	12	10	56
23	247	10	86	11	3	180
		20	258	12	3	148
		40	441	12	3	113
24	250	10	77	10	10	188
		20	317	21	10	148
		40	300	13	10	111
		48	310	20	10	102

a

b

Fig. 4. Analysis of effluent fluids: (a) conductivity measurements; (b) residual fines after produced fluid evaporation to be submitted to XRD analysis.

fines are not lifted at such low velocity, low pH and high salinity. Afterwards, the cores are submitted to the low velocity flow with the rate varying from 0.5 to 2.0 mL/min for determining the stable initial permeability. Subsequently, the cores are flooded with several rates sequentially (Table 2). The first flood is always performed with the rate 1 mL/min during short period where the permeability remains constant. Pressure at the core inlet, outlet and in two intermediate ports is measured during the coreflooding (see the schematic in Fig. 2). Measurements of pressure in intermediate core points provide more information for tuning the mathematical model and also allow estimating the permeability profile (Bedrikovetsky et al., 2001). The produced fluid salinity is determined from electric conductivity (Fig. 4a). The produced fluid pH is also measured.

The breakthrough concentrations of produced fines are too low to be measured with certain accuracy. Therefore, the fines have been removed from the core with high breakthrough concentration after water injection with three rates by injection of low salinity water (0.5 g/L). Fig. 4a shows semi-transparent effluent suspension with significant turbidity. Particle size distribution in the effluent suspension is measured by the Particle Analyser CILAS 1180 (Fig. 5). Then the produced water is evaporated in order to extract fine particles (Fig. 4b). Mineralogy of the fines is determined by XRD analysis (Fig. 6).

The obtained laboratory data are presented in the next section.

4. Results

Particle size distribution as obtained from the effluent suspension (Fig. 4a) is presented in Fig. 5. Diameters corresponding to 10%, 50% and 90% cuts are 0.38 μm, 1.35 μm and 5.03 μm, respectively; the medium particle diameter is 2.14 μm. The core permeability is $k_0 = 247$ mD, porosity is $\phi = 0.20$. The medium pore diameter is $D_p = 10 \times (k/\phi)^{1/2} = 11.1$ μm (see Amix et al. (1964) for determining pore size from the permeability and porosity). According to the "golden rule of filtration", the particles with diameter less than $D_p/7$ filtrate without being captured, the particles with diameter larger than $D_p/3$ are captured after migration for a distance that is negligibly smaller than the core length and do not appear at the effluent and the intermediate size particles are performing the deep bed filtration (Van Oort et al., 1993). The fines size distribution in Fig. 5 shows that a significant fraction of fines has the diameter less than $D_p/7 = 1.6$ μm; the fraction of large particles with diameter above $D_p/3 = 3.7$ μm is
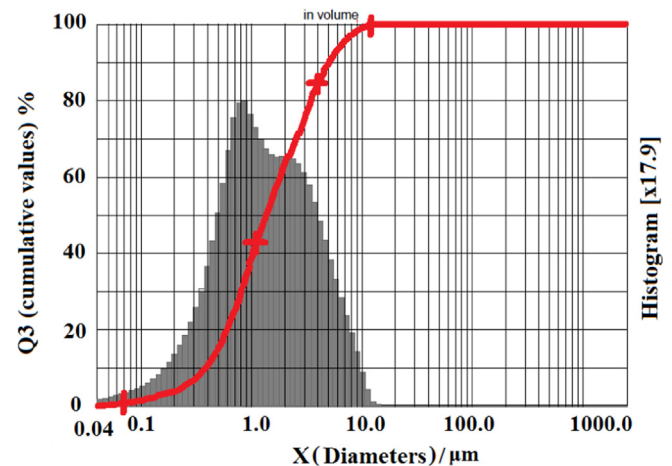

Fig. 5. Size distribution of produced fines.

significantly lower than one. The jamming ratio between the mean pore and particle diameters in the effluent 11.2/2.14 = 5.1 is typical for deep bed filtration (Bradford et al., 2008, 2009, 2011).

The dry residue of the evaporated produced suspension (Fig. 4b) is submitted to XRD analysis. The qualitative results are shown in Fig. 6. Besides the salt crystals, the residue contains the leaflets of kaolinite clay and quartz particles from sandstones. Salt presence is attributed to the injected brine. The data refinement shows 79 mass% of NaCl crystals, 18% of kaolinite and 3% of quartz.

The results of pressure measurements are shown in Fig. 7. Rates 10, 20 and 30 mL/min have been applied in Test 12. The so-called dimensionless impedance is used to describe medium permeability of different core sections

$$J(t_D) = \frac{\Delta p(t_D)}{q(t_D)} \frac{q(0)}{\Delta p(0)} = \frac{k_0}{k(t_D)}; \quad \Delta p(t_D) = p(0, t_D) - p(L, t_D)$$

where p is pressure, q is rate, the sign Δ corresponds to the difference between the upstream and downstream pressure values. The impedance is the ratio between the initial and current permeability values. The impedance history $J(t_D)$ for the overall core and its sections is presented in Fig. 7a. The pressure drop across the overall core and its sections is shown in Fig. 7b. Fig. 7c–e correspond to time zoom from the beginning of injections with a constant rate.

Let us define the pressure drop/permeability stabilisation time. The typical time interval between two sequential samplings is 10 PVI for the rates used in the coreflood tests. The precision of
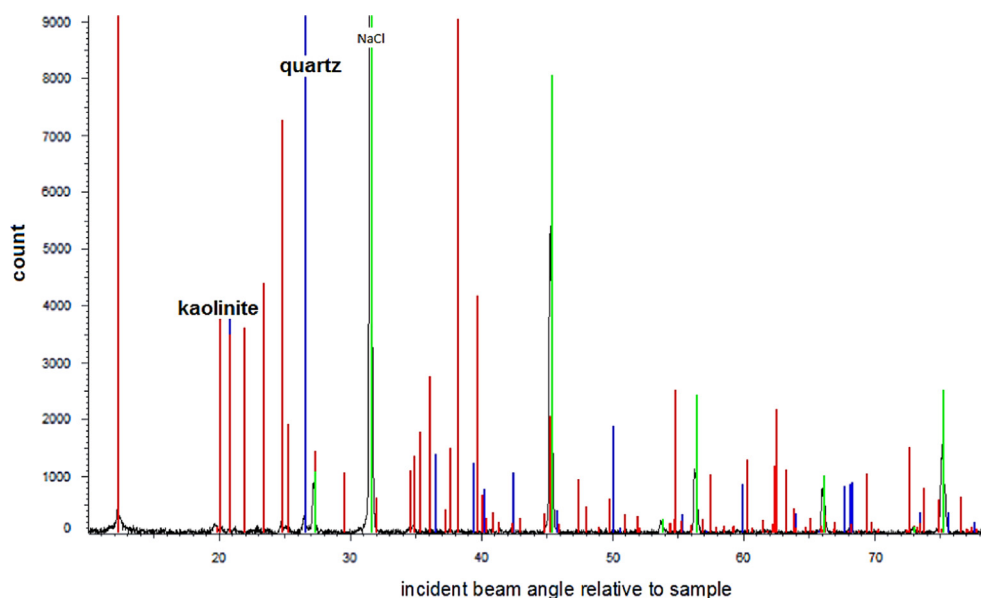
Fig. 6. Results of XRD analysis of the fines from produced fluid.

pressure measurements is 0.5 psi. The system is stabilised if the pressure drop does not grow anymore. The following criterion is assumed for stabilisation – pressure drop rise divided by the time between two sequential samplings does not exceed 0.5/10 psi. The calculated stabilisation times t_{Dst}, $J(t_{Dst})=J_{st}$ are shown in the fifth column of Table 2. Column seven presents the stabilised permeability as calculated from the stabilised impedance. The plots of permeability versus velocity for Test 12 are shown in Fig. 8. Stabilisation times versus velocity as obtained from all tests listed in Table 2 are shown in Fig. 9.

5. Discussions

The size distribution of produced fines is in qualitative agreement with the 1/3–1/7 filtration rule. It corresponds to the possibility for mobilised particles to migrate along the core and be produced at the effluent. It allows attributing the pressure drop increase during the constant rate flow to pore straining and rock clogging by the mobilised and migrating fines.

Numerous laboratory studies indicate simultaneous presence of clay and sandstone particles in produced water residue after evaporation (Lever and Dawe, 1984; Khilar and Fogler, 1998). XRD analysis of the residue fines presented in Fig. 6 also shows the presence of kaolinite clay and quartz sandstone particles.

The impedance curves in Fig. 7 indicate almost instant permeability response to the abrupt permeability alteration. So, the fine particles detachment occurs during time periods that are negligibly shorter than flow times. Fig. 7b shows pressure drop along the core, its third section and across Sections 2 and 3. Fig. 7c–e presents zoom-in for each constant rate injection during small time period from the beginning of each injection. Pressure drop gradually increases during each constant-rate injection for core and all sections; the gradual permeability decrease is explained by fines migration and straining.

The stabilised values of permeability for the overall core and its sections are shown in Fig. 8. The higher is the flow rate the lower is the permeability. It is explained by accumulation of strained particles sequentially mobilised under the increasing flow rate.

Fig. 7 shows that the impedance curve for the third core section is above that for the second and third sections; the overall core

impedance curve is the lowest. Consequently, the average permeability of the overall core is higher than that for the second and third sections; the third section has the lowest permeability. The same relationship is revealed from Fig. 8, which shows the stabilised permeability of the core and its sections after long-term injection. Let us explain the phenomenon. The mobilised fines move along the core with a certain speed. This is the velocity of the clean water front moving from the core inlet along the core from the beginning of injection. Particle size exclusion causing permeability reduction is going on ahead of the front, the suspended fines are absent behind the front. The larger is the distance between the core inlet and a point in the core, the longer is the period if particle straining occurs at this point, and the lower is the final permeability. The profile of the final permeability along the core is given by a declining curve.

Now let us discuss the obtained values of stabilisation times with consequent conclusions about the fines drift velocity. It is assumed that the fines are lifted by an abrupt velocity alternation during the time period that is negligibly smaller than the reference time of flow in the core. Therefore, the concentration front of the injected particle-free water moves with the water velocity from the core inlet at the beginning of injection. The diffusive front thickness is significantly smaller than the core length. Size exclusion of mobilised fines stops at the moment of concentration front breakthrough, i.e. after one pore volume injected. The assumption that mobilised particles are transported by carrier water results in one pore volume value for stabilisation time.

However, the observed stabilisation times highly exceed one (Table 2). It shows that the mobilised particles drift with a speed that is significantly lower than the velocity of the carrier water. This drift can be a total of different micro-motions, such as rolling over the rock surface or sliding along the pore wall segments (Yuan and Shapiro, 2010). The particle can be mobilised and move with the carrier fluid until the neighbouring asperity, either leaving it or remaining attached. The range of the transition time in PVI, which is equal to the ratio between the velocities of the carrier water and the drift, varies from 10 to 27 (Table 2).

Fig. 9 shows stabilisation time versus velocity of the carrier fluid for the conditions of all tests performed. The upper curve corresponds to the cores with higher permeability values that have been cut off the second rock block (Tests 21–24, see Table 2). The lower
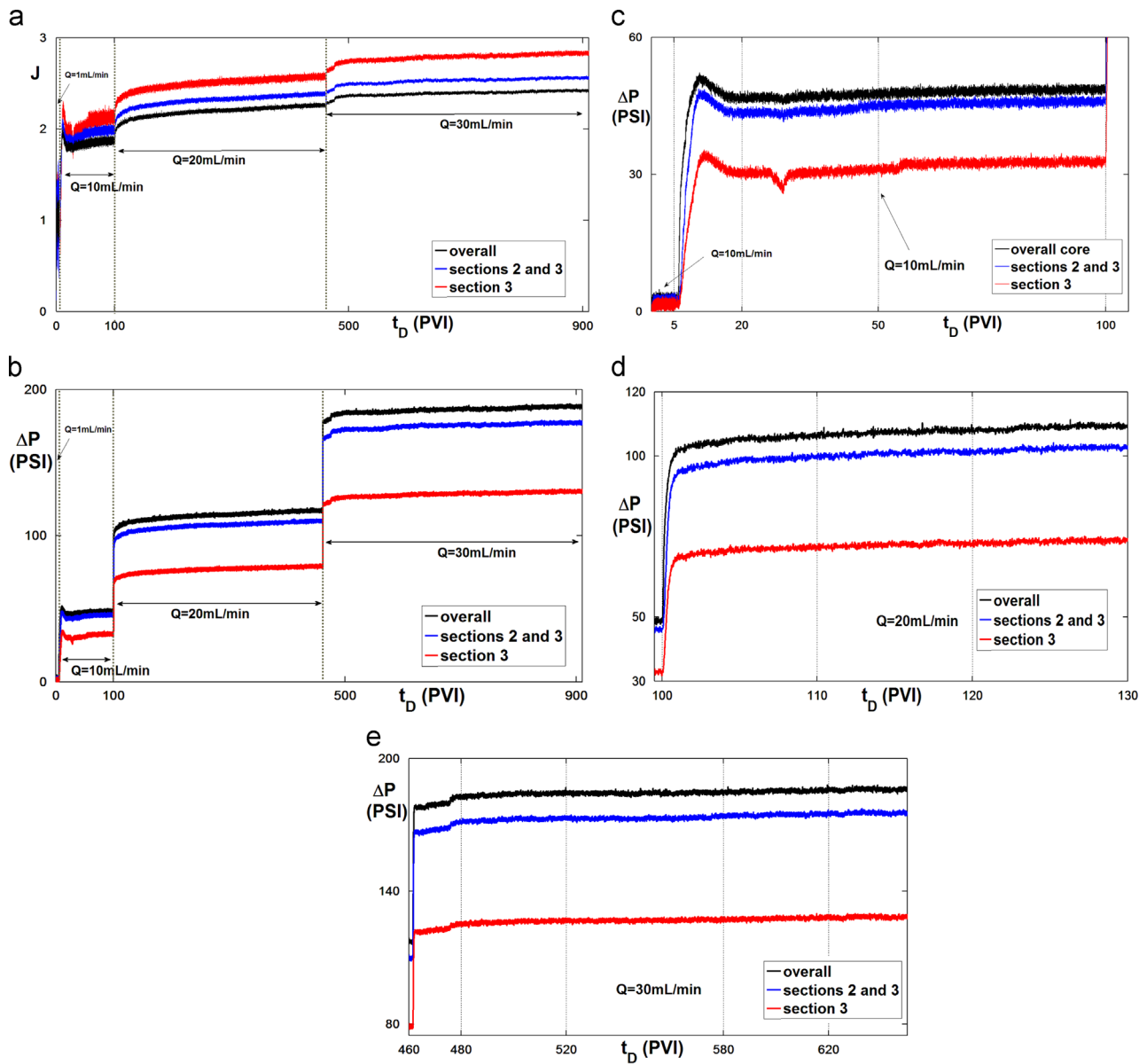
Fig. 7. Comparison of the model tuned predictions with impedance's data from Test 12: (a) impedance history; (b) pressure drops across the core and its sections versus PVI; (c) history of pressure drops across the core and its sections for rate 10 mL/min; (d) zoom for pressure drops across the core and its sections for rate 20 mL/min for small times; (e) pressure drops for rate 30 mL/min for small times.
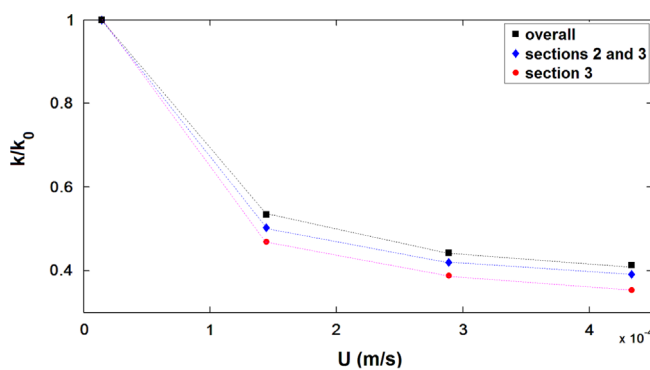

Fig. 8. Stabilised permeability versus velocity as obtained from pressure drop measurements across the overall core and its sections (Test 12).
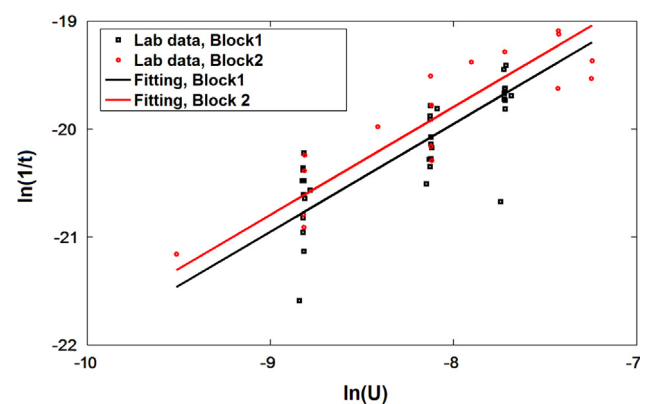

Fig. 9. Permeability stabilisation time versus flow velocity for 16 tests.

curve corresponds to the cores with lower permeability values that have been cut off the first rock block (Tests 8–20). The points are not expected to be located exactly on two curves, since the

transition times for the different points have been calculated from tests with different cores. However, the curves show the following tendency: the higher is the carrier fluid velocity, the smaller is the

transition time or, the higher is the particle drift speed. It is explained by the proportionality between the flow velocity and the drag force exerting on the particles at the rock surface.

During the injection of suspensions in porous media, the breakthrough time varies around one PVI. Small deviation of the breakthrough time from unity is explained by accessibility of the pore space for finite size particles (Ilina et al., 2008) or by the interplay between the particle capture and diffusion (Altoe et al., 2006). So, the injected particles move with the carrier fluid. On the contrary, for conditions of the laboratory tests presented in the current work, the detached particles perform a slow motion near to pore walls. Nevertheless, the above does not exclude the possibility for particle detachment into the main stream of the carrier fluid resulting in faster particle transport. It may occur at higher flow velocities and requires further laboratory investigation.

General tendency of the impedance growth during injection with velocity increase is evident from Fig. 7. However, some short time impedance decrease has been observed during the test. Fig. 7a shows the $J(t_D)$-curve decline after the rate switching from 1 mL/min to 10 mL/min. We explain it by formation of multiparticle bridges at the pore throat entrances during the induced fines migration. The abrupt rate increase may destruct the bridge and yield the fines mobilisation, resulting in a temporary permeability improvement. The effect is observed mostly at low velocities (Fig. 7). It agrees well with the above mentioned explanation of the short time impedance decline, since bridging occurs at low velocities (Tiab et al., 2004; Civan, 2007).

The explanation of permeability decline due to fines migration during the flow with increasing injection rate can be verified by applying the NMR (T2 distribution) test on each core. A possible shift in T2 distribution could be used to indicate pore plugging by the migrating fine particles (see Arns et al., 2005).

6. Conclusions

Corefloods under sequentially increasing velocity with pressure drop measurements allow drawing the following conclusions:

(1) Corefloods exhibit almost instant permeability response to abrupt rate change, suggesting that the fine particles are mobilised instantly

(2) Stabilisation time highly exceeds one pore volume, suggesting that fine particles migrate with the velocity that is significantly lower than the carrier water velocity

(3) The higher is the velocity, the lower is the stabilisation time. It is explained by the proportionality between the velocity and the drag force driving mobilised particles near to pore walls;

(4) The *post-mortem* permeability decreases along the core, since more remote core points are exposed to straining by lifted fines for longer period.

Acknowledgements

References

Amix, B., Bass, R., Whiting, A., 1964. Applied Reservoir Engineering. McGraw Hill Book Co, NY.

Arns, C.H., Knackstedt, M.A., Martys, N.S., 2005. Cross-property correlations and permeability estimation in sandstone. Phys. Rev. E 72, 046304.

Bedrikovetsky, P.G., Marchesin, D., Checaira, F., Serra, A.L., Resende, E., 2001. Characterization of deep bed filtration system from laboratory pressure drop measurements. J. Pet. Sci. Eng. 64, 167–177.

Bedrikovetsky, P., Siqueira, F.D., Furtado, C., de Souza, A.L.S., 2011. Modified particle detachment model for colloidal transport in porous media. J. Transp. Porous Med. 86, 353–383.

Bedrikovetsky, P., Zeinijahromi, A., Siqueira, F.D., Furtado, C., de Souza, A.L.S., 2012. Particle detachment under velocity alternation during suspension transport in porous media. J. Transp. Porous Med. 91 (1), 173–197.

Bergendahl, J., Grasso, D., 2000. Prediction of colloid detachment in a model porous media: hydrodynamics. Chem. Eng. Sci. 55, 1523–1532.

Bradford, S., Torkzaban, S., 2008. Colloid transport and retention in unsaturated porous media: a review of interface-, collector-, and pore-scale processes and models. Vadose Zone J. 7, 667–681.

Bradford, S., Kim, H., Haznedaroglu, B., Torkzaban, S., Walker, S., 2009. Coupled factors influencing concentration-dependent colloid transport and retention in saturated porous media. Env. Sci. Technol. 43, 6996–7002.

Bradford, S., Torkzaban, S., Wiegmann, P., 2011. Pore-scale simulations to determine the applied hydrodynamic torque and colloidal mobilisation. Vadose Zone J. 10, 252–261.

Byrne, M., Waggoner, S., 2009. Fines migration in a high temperature gas reservoir – laboratory simulation and implications for completion design. SPE 121897. In: Proceeding of the SPE 8th European Formation Damage Conference. Scheveningen, The Netherlands, 27–29 May.

Byrne, M., Slayter, A., McCurdy, P., 2010. Improved selection criteria for sand control: when are "Fines" fines? SPE 128038. In: Proceedings of the SPE International Symposium and Exhibiton on Formation Damage Control. Lafayette, Louisiana, USA, 10–12 February.

Chauveteau, G., Nabzar, L., Coste, J., 1998. Physics and modeling of permeability damage induced by particle deposition. SPE 39463. In: Proceeding of the SPE Formation Damage Control Conference. Lafayette, Louisiana, USA, 18–19 February, pp. 409–419.

Civan, F., 2007. Reservoir Formation Damage: Fundamentals, Modeling, Assessment, and Mitigation. Gulf Professional Publishing, Elsevier, Burlington.

Civan, F., 2010. Non-isothermal permeability impairment by fines migration and deposition in porous media including dispersive transport. J. Transp. Porous Med. 85, 233–258.

Freitas, A., Sharma, M., 2001. Detachment of particles from surfaces: an Afm study. J. Colloid Interface Sci. 233, 73–82.

Hussein, F., Zeinijahromi, A., Bedrikovetsky, P., Cinar, Y., Badalyan, A., Carageorgos, T., 2013. An experimental study of improved oil recovery through fines-assisted waterflooding. J. Pet. Sci. Eng. 109, 187–197.

Ilina, T., Panfilov, M., Buès, M., Panfilova, I., 2008. A pseudo two-phase model for colloid facilitated transport in porous media. J. Transp. Porous Med. 71 (3), 311–329.

Khilar, K., Fogler, H., 1998. Migrations of Fines in Porous Media. Kluwer Academic Publishers, Dordrecht/London/Boston.

Kuhn, M., Vernoux, J.F., Kellner, T., Isenbeck-Schroter, M., Schulz, H., 1998. Onsite experimental simulation of brine injection into a clasticreservoir as applied to geothermal exploitation in Germany. Appl. Geochem. 13 (4), 477–490.

Lever, A., Dawe, R., 1984. Water-sensitivity and migration of fines in the Hopeman sandstone. J. Pet. Geol. 7, 97–107.

Miranda, R.M., Underdown, D.R., 1993. Laboratory measurement of critical rate: a novel approach for quantifying fines migration problems. SPE 25432. In: Proceeding of the SPE Production Operations Symposium. Oklahoma City, Oklahoma, USA, 21–23 March.

Morrow, N., Buckley, J., 2011. Improved oil recovery by low-salinity waterflooding. J. Pet. Technol. 63 (5), 106–112.

Muecke, T.W., 1979. Formation fines and factors controlling their movement in porous rocks. J. Pet. Technol. 32 (2), 144–150.

Nabzar, L., Chauveteau, G., Roque, C., 1996. A new model for formation damage by particle retention. SPE 1283. In: Proceeding of the SPE Formation Damage Control Symposium. Lafayette, Louisiana, USA, 14–15 February.

Ochi, J., Vernoux, J.-F., 1998. Permeability decrease in sandstone reservoirs by fluid injection: hydrodynamic and chemical effects. J. Hydrol., 208 pp. 237–248.

Pang, S., Sharma, M.M., 1997. A model for predicting injectivity decline in water-injection wells. SPEFE 12, 194–201.

Priisholm, S., Nielsen, B.L., Haslund, O., 1987. Fines migration, blocking and clay swelling of potential geothermal sandstone reservoirs, Denmark. SPE Form. Eval. June, 168–178.

Rousseau, D., Latifa, H., Nabzar, L., 2008. Injectivity decline from produced-water reinjection: new insights on in-depth particle-deposition mechanisms. SPE Prod. Oper. 23, 525–531.

Sarkar, A., Sharma, M., 1990. Fines migration in two-phase flow. J. Pet. Technol. May, 646–652.

Schembre, J.M., Kovscek, A.R., 2005. A mechanism of formation damage at elevated temperature. J. Energy Resour. Technol., ASME Trans. 127 (3), 171–180.

Sefriouri, N., Ahmadi, A., Omari, A., Bertin, H., 2013. Numerical simulation of retention and release of colloids in porousmedia at the pore scale. J. Colloids Surf. A: Phys. Eng. Asp. 427, 33–40.

Sharma, M.M., Yortsos, Y.C., 1987. Fines migration in porous media. AIChE J. 33, 1654–1662.

Altoe, J.E., Bedrikovetsky, P.G., Siqueira, A.G., de Souza, A.L., Shecaira, F., 2006. Correction of basic equations for deep bed filtration with dispersion. J. Pet. Sci. Eng. 51, 68–84.

Schechter, R.S., 1992. Oil Well Stimulation. Prentice Hall, Englewood Cliffs, New Jersey p. 602.

Tang, G., Morrow, N., 1999. Influence of brine composition and fines migration on crude oil/brine/rock interactions and oil recovery. J. Pet. Sci. Eng. 24 (2–4), 99–111.

Tiab, D., Donaldson, E.C., Knovel, 2004. Petrophysics: Theory and Practice of Measuring Reservoir Rock and Fluid Transport Properties. Gulf Professional Publishing, MA, USA.

Valdya, R., Fogler, H., 1992. Fines migration and formation damage: influence of pH and ion exchange. SPEPE 7, 325–330.

Van Oort, E., Van Velsen, J.F.G., Leerlooijer, K., 1993. Impairment by suspended solids invasion: testing and prediction. SPE Prod. Facil. August, 178–184.

Watson, R.B., Viste, P., Kaageson-Loe, N., Fleming, N., Mathisen, A.M., Ramstad, K., 2008. Smart Mud Filtrate: An Engineered Solution To Minimize Near-Wellbore Formation Damage Due to Kaolinite Mobilization Laboratory and Field Experience–Oseberg Sør. SPE paper 112455 presented at 2008 SPE Formation Damage Control Conference and Exhibition, Lafayette, Louisiana, February 13–15.

You, Z., Badalyan, A., Bedrikovetsky, P., 2013. Size-exclusion colloidal transport in porous media – stochastic modeling and experimental study. SPE J. 18, 620–633.

Yuan, H., Shapiro, A., 2010. A Mathematical model for non-monotonic deposition profiles in deep bed filtration systems. Chem. Eng. J. 166, 105–115.

Yuan, H., Shapiro, A., You, Z., Badalyan, A., 2012. Estimating filtration coefficients for straining from percolation and random walk theories. Chem. Eng. J. 210, 63–73.

Yuan, H., Shapiro, A.A., 2011. Induced migration of fines during waterflooding in communicating layer-cake reservoirs. J. Pet. Sci. Eng. 78 (3–4), 618–626.

Zeinijahromi, A., Lemon, P., Bedrikovetsky, P., 2011. Effects of induced migration of fines on water cut during waterflooding. J. Pet. Sci. Eng. 78, 609–617.

Zeinijahromi, A., Vaz, A., Bedrikovetsky, P., 2012. Well impairment by fines production in gas fields. J. Pet. Sci. Eng. 88–89, 125–135.